J Intell Robot Syst (2017) 87:231–246
DOI 10.1007/s10846-017-0503-z

A New Directional-Intent Recognition Method for Walking Training Using an Omnidirectional Robot

Yina Wang · Shuoyu Wang

Received: 28 July 2016 / Accepted: 26 January 2017 / Published online: 23 February 2017

Abstract In order to avoid being bedridden, a preemptive walking rehabilitation is essential for people who lose their walking ability because of illness or accidents. In a previous study, we developed an omnidirectional walking training robot (WTR), the effectiveness of which in rehabilitation was validated by clinical testing. In the primary stage of the walking training, the WTR guides the user to follow the predesigned therapy program to conduct the walking training. This study focuses on the later stages of training in which the user plays an active role of determining the training by himself/herself, and the WTR must follow the user's intent. However, identifying a user's intent is challenging. In the present study, we address this problem by introducing a directional-intent identification method based on a distance-type fuzzy reasoning algorithm. The effectiveness of the directional identification method is experimentally confirmed.

Keywords Walking training robot · Distance fuzzy reasoning algorithm · Modus ponens · Directional intent recognition

Y. Wang (✉) · S. Wang
School of Systems Engineering, Kochi University of Technology, Kami, Kochi, Japan
e-mail: wang.yina@kochi-tech.ac.jp

1 Introduction

An increasing number of people suffer from walking disabilities caused by age, illness, or accidents [1–3]. To avoid people suffering from such problems becoming bedridden or worse, it is necessary to help them regain their ability to walk as quickly as possible through training [4]. Early rehabilitation is often achieved through training [5] and self-administered exercise regimes that can provide sufferers the option of living outside institutional care facilities [6]. Effective walking training requires not only a forward motion but also a complex combination of motions including back/forward motion, oblique motion, and rotation because that human walking inherently involves this full range of motions. However, the training devices currently in use, such as canes [7], crutches [8], parallel bars, and walkers [9], allow only a few basic motions and training primarily conducted at hospitals under the guidance of therapists. Wearable exoskeletons have been attracting interest as training systems because they offer a number of potential advantages, such as allowing the user to traverse irregular surfaces [10, 11]. Because this kind of rehabilitation device surrounds the whole leg, its motion naturally follows that of the subject [12]. However, current designs are difficult to put on and pose a danger of the user falling. Other kinds of wearable gait-training robots are popular because they can physically support the limbs during therapy and allow a more seamless transition between assistive and resistive rehabilitation as the patient progresses [13, 14]. However, these devices are expensive, cannot traning the balance of walking for users, and are only available in a restricted number of clinical or rehabilitation centers [15].

To address the convenience of walking trainers in practical applications, the authors previously developed an omnidirectional walking training robot (WTR) [16], the effectiveness of which was confirmed via clinical tests [17–19]. Our WTR can provide two levels of training, reflecting the user's walking ability as “passive walking pattern training” and “active walking pattern training”. Passive walking pattern training is the primary stage in which the training must be conducted under the guidance of therapists. Our WTR can store the training courses designed by the therapist and conduct the training courses in the absence of a therapist. The user needs to follow the WTR to continue rehabilitation, and the training course can be updated to follow up the recovery of the user. As rehabilitation proceeds, training can move to the second level, active walking pattern training. At this point, the user can independently walk and train by following the state of their own lower limbs. However, the danger of falling remains with potentially serious health consequences for the user. Our WTR therefore play a fall prevention function at this stage by moving along with the user. The user's own intent guide this motion, which mean the user plays an active role. This naturally means that the WTR must first detect the user's intent.

Handle manipulation, for example, with a mouse or joystick, could be used to communicate the user's intent to the WTR, but in such methods, the user must concentrate on the handle, which creates a danger when walking [20]. A control interface is required that is able to detect the user's directional intent without handle manipulation. Previous studies have explored a wide variety of recognition methods. One approach is based on the brain-computer interface (BCI), in which the brain activity is measured during use. These approaches mainly rely on electroencephalography (EEG), which is safe and inexpensive but has slow communication [21]. Magnetoencephalography (MEG) offers a higher signal quality and communication speed than EEG, but it is too expensive for personal use in domestic settings [22]. Functional magnetic resonance imaging (fMRI) [23, 24] is also expensive and has high variability in measurement of brain signals, as does functional near-infrared spectroscopy (fNIRS) [25]. All these BCI methods are in the early stages of research and development and are not yet sufficiently mature for practical applications. Motion intentions can also be communicated by explicit voice commands from the user [26], but this is inconvenient since the clear expression of directional intentions is difficult. This method can only cover a restricted range of directional intent as it uses a discontinuous method of expression. Other approaches used robot vision [27, 28], including depth vision sensors, to estimate the user's walking state when requiring assistance [29]. The accuracy of this method is low, and this method is difficult to apply to the WTR which we developed. In [30], an inertial measurement unit (IMU) was used to infer the directional intentions of the user. However, the accuracy was insufficient due to the drift of the internal sensor. Electromyography (EMG) has been used extensively to detect user's intent [31]. The recognition rate of this method is low due to its high sensitivity to electrode displacement [32]. An interface “plate” was developed to indicate directional intent [33]. and in some other approaches, the handles of the walker were equipped with 6-DOF force/moment sensors [34] or a six-axis force/torque sensor was used to create an interface between the user and an omnidirectional cane robot [35]. The essential principle of these methods, however, is the same as the principle using a joystick to guide an electric wheelchair, which was developed without considering the user and only focusing upon the basic mechanical functions of the robot. In application, since there are individual differences, all users must familiarize themselves with the same manipulation technique for the robot. Therefore, these methods still require the user to strictly concentrate on the manipulation of the handle, which can be inconvenient or dangerous when walking.

Artificial intelligence (AI) is a quite effective way to improve the robot intelligence to conveniently estimate the intent of the user. In recent years, AI has been used in a wide range of fields including medical diagnosis, stock trading, robot control, drilling system, smart grid, and buildings [36, 37]. Most of these applications have validated that AI is successful and useful in these filed. For example, for application in the forecasting of the Dez reservoir inflow,

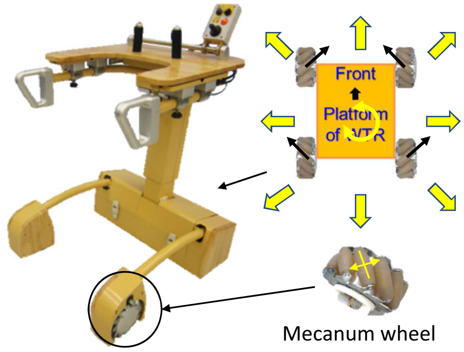

Fig. 1 Walking training robot

the method of autoregressive ANN is verified to be more superior than the method of ARMA and ARIMA [38]. Moreover, the method of dynamic autoregressive ANN is the best way to forecast the inflow [39], the application in pressure loss adjusting for the design of sprinkle and trickle irrigation system [40], the application in simulation of surface irrigation using SIRMOD [41], and the contrast of these surface irrigation simulation models to design and manage the irrigation systems [42]. These successful application cases could be as the reference and contrast for us. Therefore, we develop the directional intent recognition method for the WTR based on the AI.

In this paper, we proposed a novel intelligent method for recognizing a user's intended direction based on a distance-type fuzzy-reasoning method. The key contribution to this approach is very comfortable and intuitive for the user, as it considers the users' individual operational characteristics, its ease of implementation, its high identification accuracy compared to other method. This method can be applied to users with different walking habits by updating the fuzzy knowledge base. This base is a simple and intuitive method for quantitatively expressing the relation between the force-sensor outputs and directional intent based on the concept of using vague linguistic variables. In addition, a distance-type fuzzy-reasoning method is proposed to determine the directional intent. Even if there are no intersection between the fuzzy knowledge base and the fact meaning the present force outputs, this method is still effective. The effectiveness of the proposed method was validated though a series of experiments.

2 Method

2.1 Walking Training Robot

We first constructed a prototype of our WTR, which has been designed to fasten the recovery of walking ability. Four powered mecanum wheels were positioned in the configuration shown in Fig. 1, enabling omnidirectional movement of the WTR [16]. The four wheels were independently driven by four highly efficient, permanent, magnet-activated direct current (DC) motors controlled by a servo controller [43]. The upper limit to payload for each mecanum wheels is 80kg, maximum loading range is from 11kg to 80kg, and the power source is DC 24V. Supported by the WTR, a test user could move through an indoor environment by resting his or her arm on the armrest (Fig. 2). Four uniaxial force sensors labeled Sen.FL, Sen.FR, Sen.BL, and Sen.BR (where F, L, B, and

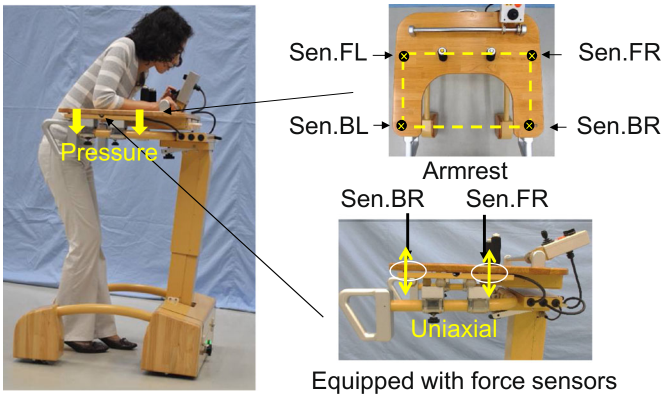

Fig. 2 Walking training robot used for walking assistance

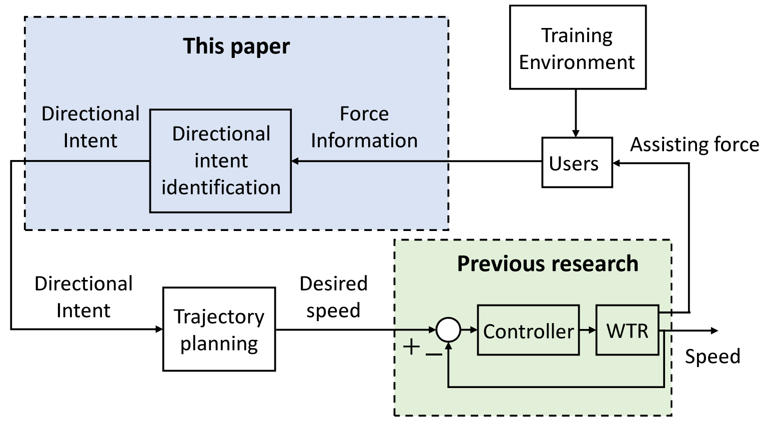

Fig. 3 The total walking rehabilitation system

R denote front, left, back, and right, respectively) to measure the pressure from user were installed at the four support points between the WTR's armrest and body, as shown in Fig. 2. These positions represent the main user-robot interfaces. When assume that the pressure applied by the user acts at the center of the four points, all loads are uniformly borne by the four support points while the user's arms are on the armrest. Consequently, force sensors at these four points can be used to distinguish a user's directional intent.

The complete functioning of the walking rehabilitation system is shown in Fig. 3. As the user chooses a walking direction and consciously inclines his or her body in that direction, the WTR identifies the user's intent by sensing the forces applied to the armrest. The speed of the WTR is generated using a trajectory planning method according to the identified intent. And we will develop the trajectory planning method in our future worker. A controller was proposed to ensure the tracking accuracy of the WTR, as described in our previous report [44]. Finally, the WTR assists the user to move in the intended direction. In this study, we focused on developing the identification of directional intent.

2.2 Mechanism of our Directional-Intent Recognition Method

When approaching one direction, the human body is naturally inclined in the targeted direction. We exploited this observation to detect the user's directional intent. For example, when a user wants to move to the left while standing at the center of the WTR (Fig. 4), his or her body inclines in the intended direction while the arms press on the armrest to prevent falling. The distribution of forearm pressure on the four sensors then changes, allowing the directional intent to be inferred from the change in the distribution of pressure.

Our distance-based fuzzy-type reasoning method needs the fuzzy linguistic variables (For examples: large, medium, small, and very small) to express the outputs of the force sensors. The user was assumed to travel in eight directions: Right (R), Front Right (FR), Front (F), Front Left (FL), Left (L), Back Left (BL),

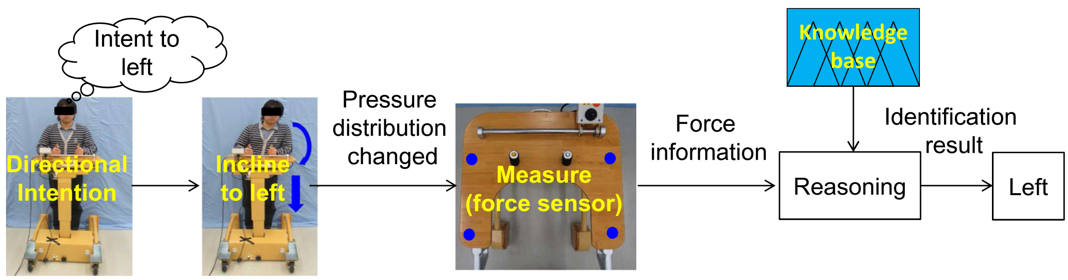

Fig. 4 Identify method: with the left intention

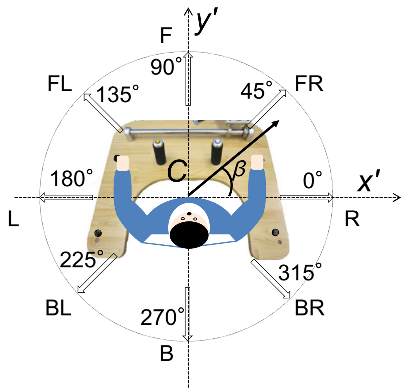

Fig. 5 Subject's required direction and angle in experiment

Back (B), and Back Right (BR). The eight directions were defined by eight angles in the robot's body coordinate system, as shown in Fig. 5. The directional intent was defined as β with respect to the x'-axis in the WIR's body coordinate system. The relationship between the directional intent and the outputs of the force sensors is described using fuzzy logic for the following cases as some general examples.

Case 1 When the user wants to move toward the front right, the output of Sen.FR is large, the output of Sen.FL is small, the output of Sen.BR is small, and the output of Sen.BL is very small.

Case 2 When the user wants to move toward the left, the output of Sen.FR is very small, the output of Sen.FL is medium, the output of Sen.BR is very small, and the output of Sen.BL is medium.

Case 3 When the user wants to move back, the output of Sen.FR is very small, the output of Sen.FL is very small, the output of Sen.BR is medium, and the output of Sen.BL is medium. A total of 256 cases are obtained by the different combinations of the four sensors because each sensor has four conditions. The resulting angular resolution is less than 1.5°, which is less than the angular resolution of the human eye. Consequently, four force sensors at the four orthogonal directions of the WTR's armrest are sufficient to distinguish a user's directional intent. This allows the user's directional intent to be inferred with high accuracy as follows:

If Sen.FR is large, Sen.FL is small, Sen.BR is small, and Sen.BL is very small, then β is 45°.

If Sen.FR is very small, Sen.FL is medium, Sen.BR is very small, and Sen.BL is medium, then β is 180°.

If Sen.FR is very small, Sen.FL is very small, Sen.BR is medium, and Sen.BL is medium, then β is 270°.

However, the directional intent and the physical representation of that intent do not always match because of the distinctly individual habits of human movement and because the settings of the four sensors are not identical. In the next subsection, we introduce the development of the knowledge base for the fuzzy logic system and the characterization of the linguistic variables on the basis of their membership functions.

2.3 Constructing the Membership Functions of the Linguistic Variables

As noted above, the outputs of the four force sensors cannot be uniformly described using only four conditions. We therefore experimentally collected a knowledge base and determined the membership functions of the linguistic variables for different individuals. In our experiments, users were asked to consciously orient themselves in eight separate directions, as shown in Fig. 5, while remaining stationary. Each user briefly inclined his or her body in each direction across several trials. The mean and standard deviation (SD) of each sensor output in each direction was calculated and labeled as $A^{ij}.Mean$ and $A^{ij}.SD$, where, i= 1, 2,..., 8 denote the number of directional intent, j=1, 2, 3, 4 denote the number of sensor. Here, A^{ij} is a linguistic variable of each sensor in each direction, and $\mu_{A^{ij}}(x)$ is the membership function of each variable. A membership function $\mu_{A^{ij}}(x)$ was represented by the normal triangular fuzzy set shown in Fig. 6 with parameters a_1^{ij}, a_2^{ij}, and a_3^{ij}, which were calculated from the means and SDs of the sensor outputs: $a_1^{ij} = A^{ij}.mean - A^{ij}.SD$, $a_2^{ij} = A^{ij}.mean$, and $a_3^{ij} = A^{ij}.mean + A^{ij}.SD$. The singleton set A^j represents one parameter a^j which denotes the current output of each sensor, where $\mu_{A^j}(x)$ is the linguistic variable of

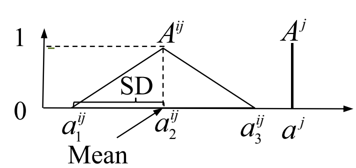

Fig. 6 Definition of Linguistic variables' membership functions

fact A^j, and B^i is the linguistic variable representing the user's directional intent. Also, $\mu_{B^i}(x)$ is the membership function of B^i, which is a singleton set with one parameter b^i.

Then, the if-then fuzzy rules are extracted as Eq. 1 to govern the deduction of proposition result from a set of premises.

$$\begin{array}{llll}
\text{Rule 1: If } x_1 = A^{11}, x_2 = A^{12}, x_3 = A^{13}, x_4 = A^{14} & \text{then } \beta = B^1 \\
\text{Rule 2: If } x_1 = A^{21}, x_2 = A^{22}, x_3 = A^{23}, x_4 = A^{24} & \text{then } \beta = B^2 \\
\quad\;\vdots \qquad \vdots \qquad\quad \vdots \qquad\quad \vdots \qquad\quad \vdots & \qquad\quad \vdots \\
\text{Rule 8: If } x_1 = A^{81}, x_2 = A^{82}, x_3 = A^{83}, x_4 = A^{84} & \text{then } \beta = B^8 \\
\\
\text{Fact : } x_1 = A^1, x_2 = A^2, x_3 = A^3, x_4 = A^4 & \\
\hline
\text{Result :} & \beta = B
\end{array} \tag{1}$$

where A^{ij} and B^i $(i = 1, 2, \cdots, 8,\ j = 1, 2, 3, 4)$ are the antecedent and outcome discussed above, and A^j and B are the fact and result, respectively. The membership between antecedents x_1, x_2, x_3, and x_4 was given by AND. The sensor outputs showed that no two rules were identical. When the fuzzy rules were defined as described, the user's directional intent could be derived from the current output of the force sensors using a distance-type fuzzy reasoning method. This is described in the next subsection.

2.4 Distance-Type Fuzzy Reasoning Method

Mamdani's fuzzy reasoning [45], functional fuzzy reasoning, and simplified fuzzy reasoning are widely used in fuzzy control, expert systems, and other fields [46, 47]. This approach to fuzzy reasoning is generally called the direct approach. However, an associated problem is that the degree of compatibility between antecedent and fact is represented by the height of the common area between them as shown in Fig. 7a. This means that the fact set needs to intersect with the antecedent set. If the common area has empty parts and if the fact set is located inside those empty parts(situation in Fig. 7b), no reasoning result can be derived [48, 49].

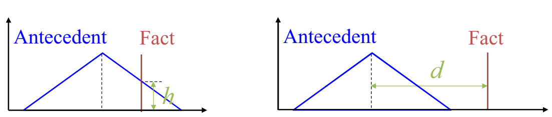

(a) Height of common area (b) Distance

Fig. 7 Difference between the (**a**) direct approach and (**b**) proposed method

In our study, there were empty common areas between the antecedent sets, and the relevance between antecedent and fact sets was therefore expressed by the distance between the two, not by their shared common area (see Fig. 7b). This makes our method effective even when the antecedent is completely separate from the fact [50]. A range of methods can be used to calculate the distance between two fuzzy sets [51, 52]. To make the calculation simple and accurate, we used a distance calculation that measures how far the two sets are from each other based on Euclidean distance [50]. For the fuzzy sets A^{ij}, A^j, the distance is calculated as

$$d(A^{ij}, A^j) = \left[\int_0^1 \left| inf A_\alpha^{ij} - inf A_\alpha^j \right|^p d\alpha\right]^{1/p} + \left[\int_0^1 \left| sup A_\alpha^{ij} - sup A_\alpha^j \right|^p d\alpha\right]^{1/p} \tag{2}$$

where $1 \leq p < \infty$; $|\cdot|$ represents calculation of the absolute value, and inf and sup refer to the lower and upper limit values of the set, respectively. A_α^{ij} and A_α^j are the α-level set of fuzzy sets A^{ij} and A^j , which are defined as, $\forall\alpha \in (0, 1]$, $A_\alpha^{ij} = \left\{x \in R | \mu_{A^{ij}}(x) \geq \alpha\right\}$, and $A_\alpha^j = \left\{x \in R | \mu_{A^j}(x) \geq \alpha\right\}$.

The proposed method of identifying directional intention based on the distance-type fuzzy reasoning method consisted of the following three steps.

Step 1: On the basis of the distance calculation method shown in Eq. 2, the distance d_{ij} between the jth antecedent triangle-type fuzzy set of the ith rule A^{ij} and the fact fuzzy singleton A^j can be calculated as

$$d_{ij}(A^{ij}, A^j) = \frac{1}{\sqrt{3}} \sum_{k=1}^{2} \left[\sum_{l=k}^{k+1} (a_l^{ij} - a^j)^2 + \prod_{l=k}^{k+1} \left| a_l^{ij} - a^j \right| \right]^{\frac{1}{2}} \tag{3}$$

where $i = 1, 2, \cdots, 8$, and $j = 1, 2, 3, 4$. Note that the distance d_{ij} requires three parameters. The calculated distance d_{ij} increases as the fact becomes further separated from the antecedent. When fact A^j exactly coincides with antecedent A^{ij}, the distance d_{ij} is 0.

Step 2: The membership between antecedents x_1, x_2, x_3, and x_4 was given by AND. Hence, the distance

d_i between the antecedent of the ith fuzzy rule and fact A^j was given by

$$d_i = \sum_{j=1}^{4} w_j d_{ij}(A^{ij}, A^j) \tag{4}$$

The value d_i shows the relevancy between the fact and the ith rule. A small d_i indicates a strong relevance, implying that the identification result is close to the ith result. In this study, w_j reflected the importance of each sensor in each fuzzy rule. Weighting the sensors improved the WTR's reasoning accuracy, which will be further explored in future work. In this study, all w_j are set to 1.

Step 3: The identified directional intention angle β was calculated by the following reasoning:

$$\beta = \frac{\sum_{i=1}^{n}[b^i \prod_{j=1, j\neq i}^{n} d_i]}{\sum_{i=1}^{n} \prod_{j=1, j\neq i}^{n} d_i} \tag{5}$$

where b^i is the consequent of each fuzzy rule. For Eq. 5, the reasoning result is the spatial average of all fuzzy consequents, in terms of relevance d_i between the fact and the fuzzy rules. A special condition is $d_i = 0$, which implies that the fact exactly equals fuzzy rule i. In this case, result from Eq. 5 is the ith fuzzy consequent, which conforms to the physical truth.

The effectiveness and the special features of the proposed distance-type reasoning method are shown as follows.

Theorem 1 *The reasoning result using distance-type reasoning is bounded.*

Proof On the basis of the distance calculation method shown in Eq. 2, $\forall k \in \{1, 2, \cdots, 8\}$, $d_k \geq 0$, and because no two antecedent sets are exactly the same, $\sum_{i=1}^{n} \prod_{j=1, j\neq i}^{n} d_i \neq 0$. Furthermore, each consequent b^i and distance d_i is bounded, based on Eq. 5; thus, β is bounded. □

Theorem 2 *The reasoning method exactly satisfies the modus ponens: $\exists i \in \{1, 2, \cdots, 8\}$ if $\forall j \in \{1, 2, 3, 4\}$ and $A^j = A^{ij}$ then the reasoning result is $\beta = b^i$.*

Proof Here, $\forall j \in \{1, 2, 3, 4\}$, if $A^j = A^{ij}$, then, based on the distance calculation method shown in equation (4), we can obtain the distance $d_i = 0$. Moreover, there are no two antecedent sets exactly the same, $\forall k \in \{1, 2, \cdots, 8\} - \{i\} \neq 0$, $d_k \neq 0$. Therefore, we get the reasoning result $\beta = b^i$. □

Theorem 3 *If the fact is closer to one antecedent, the result is closer to the consequent of that antecedent.*

Proof B is the reasoning result with distance $d_1, d_2, \cdots, d_q, \cdots, d_n$, and B' is the reasoning result with distance $d_1, d_2, \cdots, d_q{}', \cdots, d_n$. As no two antecedent sets are exactly the same, $\forall k \in \{1, 2, \cdots, 8\} - \{i\} \neq 0$, $d_k \neq 0$, if $d_q < d_q{}'$, then $d(B, B^q) < d(B', B^q)$, where B^q is the reasoning result when $d_q = 0$. Thus, when the fact is closer to one antecedent, the result is closer to the consequent of that antecedent. □

Theorems 2 and 3 show that this reasoning method satisfies the asymptotic characteristic of reasoning, in which the reasoning result is estimated in such a way that it agrees with human intuition.

3 Experiments and Results

Our experiments to validate the effectiveness of the proposed method recruited six healthy subjects (three males and three females), coded A, B, C, D, E, and F. The experimental procedures involving human subjects described in this section were approved by Kochi University of Technology, and written informed consent was obtained. The average age of the subjects was 29, the average height was 165 cm, and the average weight was 61.3 kg. All participants were healthy and had similar walking habits. We first collected the knowledge base and determined the membership function of the linguistic variables. Each subject was asked to incline his or her body in each direction for 20 s, and ten trials for each direction were conducted. The total mean and SD of the force sensor outputs as the six subjects consciously moved in eight different directions constituted the antecedent fuzzy knowledge, while the eight directional intentions formed the consequent knowledge. This is summarized in Table 1, and the membership functions of the antecedent knowledge sets are shown in Fig. 8. A^{i1} ($i = 1, 2, \cdots, 8$) denote the membership functions of the eight fuzzy variables defined as the directions R, FR, F, RL, L, BL, B, BR obtained by the Sensor.FR. Those obtained by Sensor.FL, Sensor.BR, and Sensor.BR are, respectively, denoted by A^{i2}, A^{i3} and

Table 1 Abstraction of the Fuzzy Knowledge

Rules	Sen.FR	Sen.FL	Sen.BR	Sen.BL	B^i
Mean	36.7	5.7	74.8	8.0	R(0°)
SD	22.4	3.7	10.4	6.2	
Mean	51.7	9.3	28.9	7.6	R(45°)
SD	20.9	6.3	9.3	3.2	
Mean	36.9	33.2	3.1	5.5	R(90°)
SD	11.2	11.0	11.3	10.6	
Mean	12.1	44.0	7.7	27.9	R(135°)
SD	9.0	20.4	3.1	9.2	
Mean	7.6	27.11	13.0	69.3	R(180°)
SD	3.1	10.1	13.5	13.5	
Mean	16.0	13.2	21.3	85.6	R(225°)
SD	5.8	8.8	13.2	22.1	
Mean	4.4	2.7	72.0	71.8	R(270°)
SD	4.1	5.9	25.5	28.3	
Mean	14.9	12.4	84.9	15.5	R(315°)
SD	12.4	3.1	30.1	8.8	

A^{i4}. It can be seen that the width of each membership function is different, and the distribution of the membership functions is uneven. This is because the membership functions were set up by repeated experiments based on intuitive manipulation of subjects to thoroughly express the subjects' individual differences and actual operational conditions. These variations of the membership function precisely reflect the advantages of the proposed method, which has appropriately embraced the subjects' operational characteristics. In detailed, if the target direction was FR, the user placed maximum forearm pressure on Sen.FR (compare A^{21}, A^{22}, A^{23}, A^{24}); furthermore, if the target direction was B, the user placed max forearm pressure on Sen.BR and Sen.BL (compare A^{71}, A^{72}, A^{73}, A^{74}). These graphical trends are consistent with what was observed during the actual event. On the other hand, the Sensor.FR attained its maximum values (A^{21} and A^{11}) when traveling in the FR and R direction, and its minimum values (A^{51} and A^{61})when traveling in the L and BL direction. The same tendencies were obtained with Sensor.FL, Sensor.BR, and Sensor.BL. However, on the whole, the outputs of Sensor.BR and Sensor.BL are larger than those of Sensor.FR and Sensor.FL, as the pressure of an elbow on the armrest is larger than that of a hand, due to the habits and forearm characteristics of a human being. Additionally, not all results are consistent with the normal situation due to individual differences. Therefore, the fuzzy knowledge base with the membership function introduced in this paper successfully simulates this event, as shown in Fig. 8.

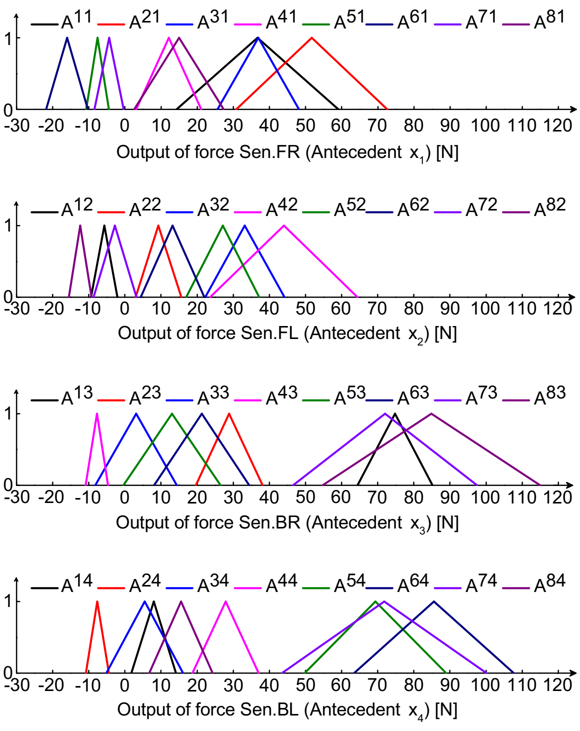

Fig. 8 Membership functions of antecedent knowledge sets

3.1 Experiment: Relationship Between Knowledge Radius and Reasoning Accuracy

It is well known that humans do not use their full range of knowledge when making inferences or judgments. Instead, they use only the knowledge that is relevant in the particular situation. If irrelevant or only slightly relevant knowledge is applied, accuracy is impaired.

In the same way, fuzzy reasoning does not utilize the entire set of antecedent knowledge in all cases. Antecedent knowledge that has little relevance to the facts at hand is disregarded. This research incorporated such selective use of knowledge, referred to as the knowledge radius. In the study, the knowledge radius r specified the number of antecedent knowledge sources that were clearly relevant to the situation at hand. In step two of the distance-type fuzzy reasoning process, the calculated distances between the

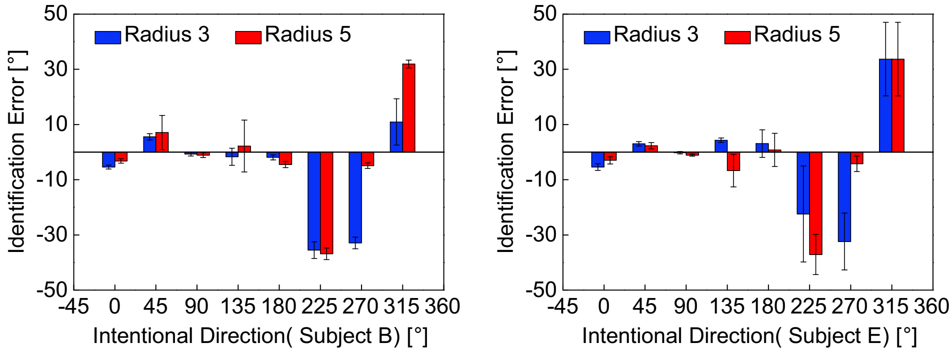

Fig. 9 Means and standard deviations of identification errors in each direction with radii of 3 and 5 (for subjects B and E)

current fact and antecedent fuzzy set were ordered and stored: the smaller the distance, the smaller the number, and the greater the relevance. The knowledge radius was accounted for in step 3, as n was replaced by the knowledge radius r in Eq. 5. Since the number of antecedent knowledge sources for directional intention fuzzy reasoning was eight, r could be set as 2, 3, $\cdots$, 8.

Subjects B and E participated in experiments designed to validate the proposed method for identifying directional intention. The two subjects were requested to remain stationary with their arms on the armrests while inclining their bodies in one of the eight target directions (Fig. 5) in an ordered sequence. Participants rested for 10 s before inclining their body in the next targeted direction for 20 s. Two trials per subject were conducted for each direction. Using the force sensor outputs and the fuzzy reasoning method detailed in Section 3 and varying the knowledge radius through all values between 2 and 8, the directional intent of each subject was determined. The means and SDs of the identification errors in each direction are shown in Figs. 9 and 10.

It can be seen that the reasoning accuracy was dependent upon the knowledge radius r. A knowledge radius which achieves high reasoning accuracy is dependent upon the directional intent. For most directions of movement (R, FR, F, FL, L), a high reasoning accuracy was achieved with knowledge radii of 3 and 5. In all directions, however, the reasoning accuracy was maximized at other knowledge radii. The knowledge radius was therefore shown to significantly affect accuracy of the proposed fuzzy reasoning method.

As shown in Figs. 9 and 10, knowledge radii of 3 and 5 minimized the identification errors of subjects B and E, and particularly improved the reasoning

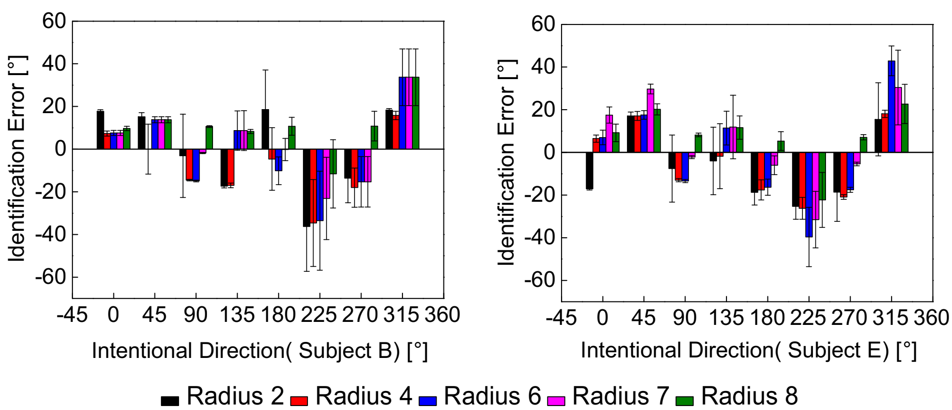

Fig. 10 Means and standard deviations of identification errors in each direction with radii of 3 and 5 (for subjects B and E)

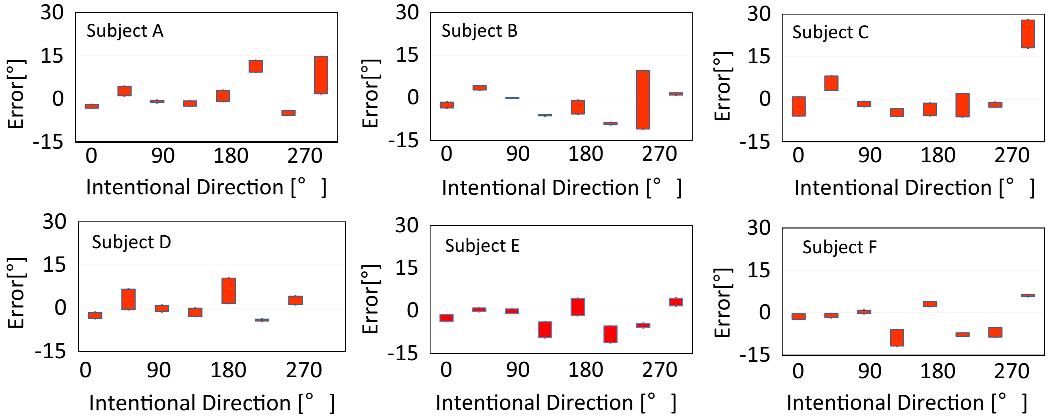

Fig. 11 Identification error of each subject

accuracies of the first five directions (R, FR, F, FL, L). The directional identification method was then further validated using a knowledge radius of 5.

3.2 Experiment: Identification Error of Each Subject

To further validate the reliability of the proposed identification method, the six subjects were requested to intentionally maneuver the robot moving straight along eight fixed directions (R, FR, F, FL, L, BL, B, BR). The knowledge radius was set as 5, and the method used was the same as that in the previous experiment. The means and standard deviations of the identification errors of each subject are shown in Fig. 11.

3.3 Experiment: Path Tracking

The third experiment was designed to verify the usefulness of the proposed method in a practical application. Experiments were conducted in an indoor environment that made the subjects to track two kinds of predefined path shown in Fig. 12. since the WTR's orientation is a constant 90°, so that the x'-axis in the WTR's body coordinate system is always the same as the x-axis in the absolute coordinate system. The angle of identified directional intention was denoted as β in the two-dimensional (2D) world coordinate system, as shown in Fig. 13, and denoted the angle of directional intention with respect to the x-axis. The velocity of the WTR was denoted by V and was set to $V = 0.3m/s$. Using the intentional direction angle β and the defined velocity V, the x- and y-components of the velocity of the WTR are given by Eq. 6.

$$\begin{cases} v_{cx}(t) = cos\beta \cdot V \\ v_{cy}(t) = sin\beta \cdot V \\ \omega = 0 \end{cases} \tag{6}$$

The required speeds for the four wheels of the WTR were derived from the kinematic model Eq. 7, following [44] .

$$\begin{bmatrix} v_1 & v_2 & v_3 & v_4 \end{bmatrix}^T = K_V(\theta) \begin{bmatrix} v_{cx} & v_{cy} & \omega \end{bmatrix}^T \tag{7}$$

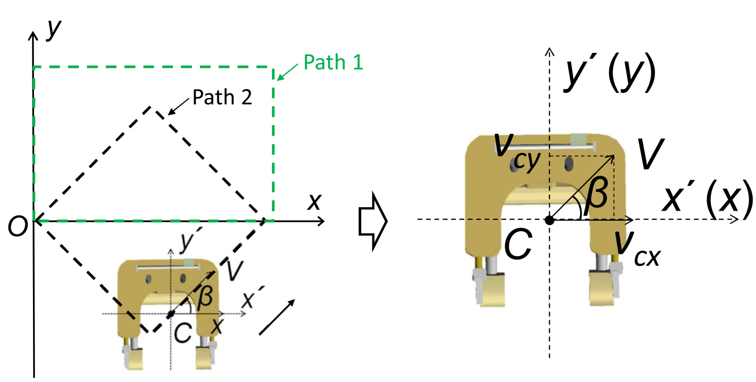

Fig. 12 The definition of the identification angle in the 2-D coordinate system

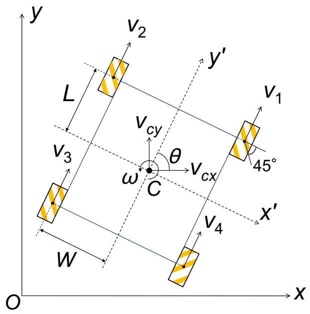

Fig. 13 Structure and vector diagram of the WTR in a 2D coordinate system

where:

$$K_V(\theta)=\begin{bmatrix} -cos(\theta)-sin(\theta) & cos(\theta)-sin(\theta) & L+W \\ cos(\theta)-sin(\theta) & cos(\theta)+sin(\theta) & -(L+W) \\ -cos(\theta)-sin(\theta) & cos(\theta)-sin(\theta) & L+W \\ cos(\theta)-sin(\theta) & cos(\theta)+sin(\theta) & -(L+W) \end{bmatrix}^T$$

As shown in a 2D coordinate system of Fig. 13, W is the half Width of WTR, L is the half Length of WTR, $v_i(i = 1, 2, 3, 4)$ are the moving speeds of four wheels, v_{cx}, v_{cy} are the x- and y-components of the WTR's velocity, respectively, and ω denotes the WTR's angular speed.

Subjects B and E, who participated in the establishment of the fuzzy knowledge base, were recruited for this experiment. The subjects first mentally mapped the path they wanted to track and then inclined their bodies in the intended direction. In doing so, their forearms exerted alternating pressure on the WTR's armrest. The angle of directional intention was identified from the measured force sensor outputs using our fuzzy reasoning method. Equations 6 and 7 were used to obtain the required speed for each of the four wheels, allowing the WTR to move in the intended direction. From the servo controller, an open-loop speed controller fed the four permanent magnet-activated DC motors with voltages proportional to the required speed. Each subject completed two trials for each path. The identification angles to track the two path for subjects B and E are shown in Figs. 14 and 15. And the tracking results for both paths are shown in Figs. 16 and 17 for these two subjects respectively. To further validate the proposed method, a healthy subject (age 27, height 166 cm, weight 59.2 kg, male) who was not involved in generating the fuzzy knowledge base was recruited for the path-tracking experiment. His intentional paths were the same as those of subjects B and E, and his identification angles and tracking results are shown in Figs. 18 and 19.

4 Discussion

Firstly, the results of experiment 3 indicate that the proposed method can be easily applied to WTR for travel in the intended direction, which is superior

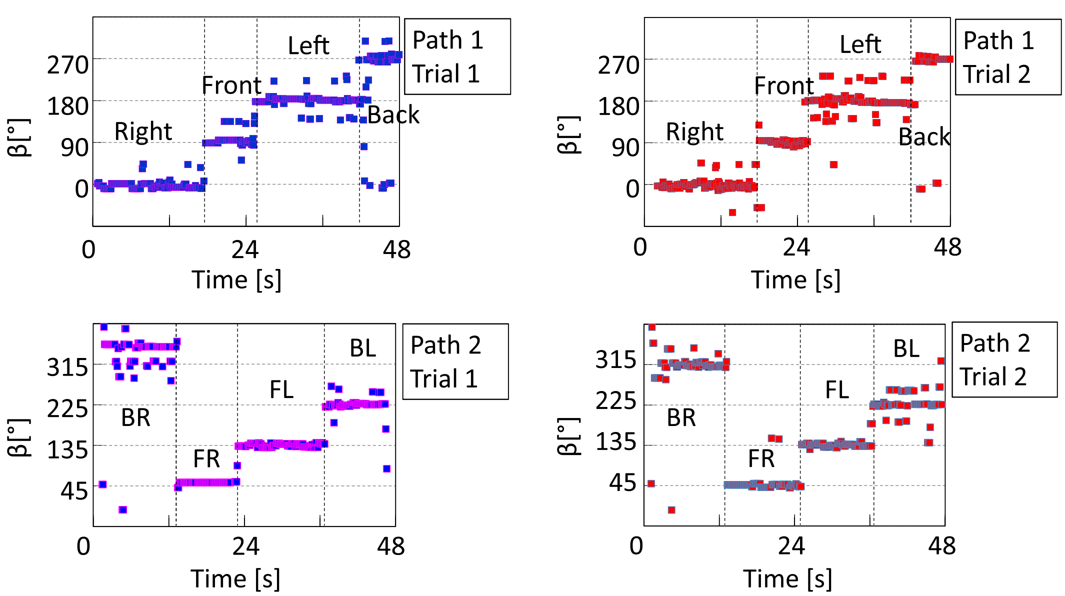

Fig. 14 Subject B's identification angles

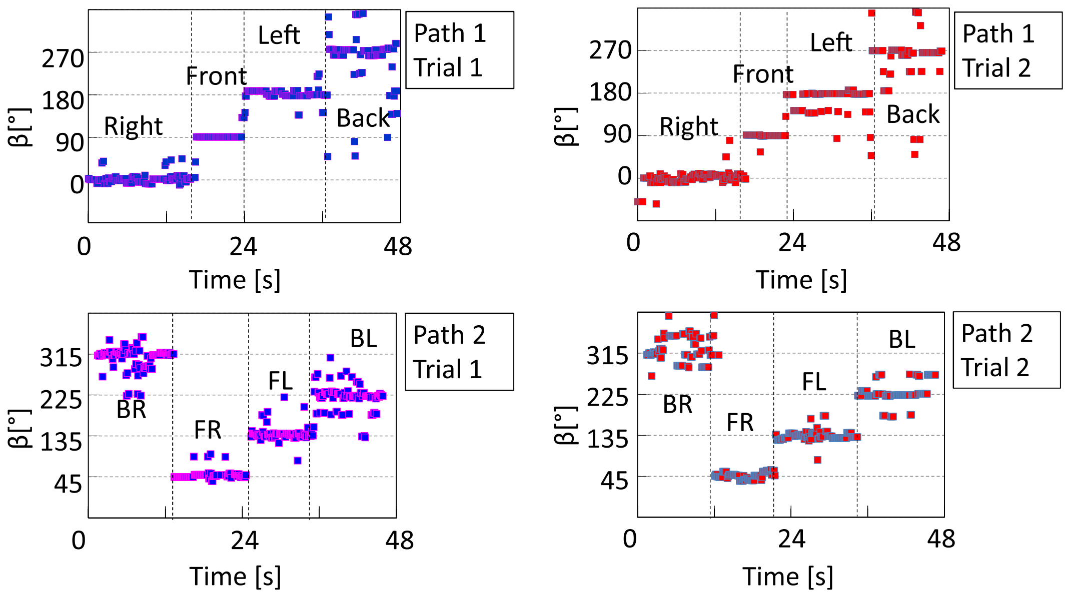

Fig. 15 Subject E's identification angles

to, and more convenient than, the methods based on fMRI, EEG, and fNRIS. All the experimental results confirmed that the proposed method was able to recognize the directional intention of the user. As shown in Fig. 11. the identification error was less than 3° in directions R, FR, and F and was less than 7°, in directions FL, L, and B. The errors were slightly larger in the other two directions. These are important results for comparing the errors with those of the methods based on IUM and EMG. There are fewer identification errors in the proposed method than in the methods based on IUM and EMG, which shows again the proposed method's superiority. The reason for this better performance is that the force sensors used in the proposed method are more stable and have less noise and drift phenomena. Besides, although identification errors were found in each direction, the results were promising and showed greater levels of accuracy than those reported elsewhere [32, 35]. Since the proposed fuzzy knowledge base drawn from linguistic variables can appropriately simulate the relation between forearm pressure and directional intent, it is more accurate than the method proposed in [32, 35].

The cause of identification errors might be related to the exact of knowledge base and reasonability of the distance-calculation method and reasoning method. The knowledge base was set-up based on the statistical results from the collection and processing of data

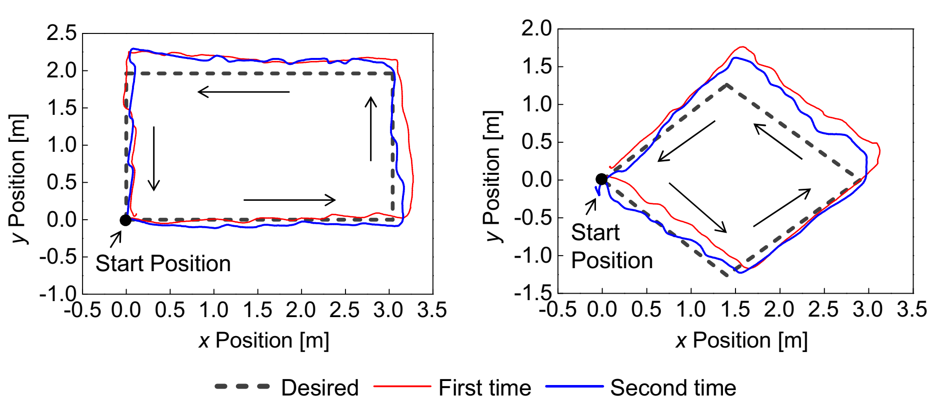

Fig. 16 Subject B's path-tracking results

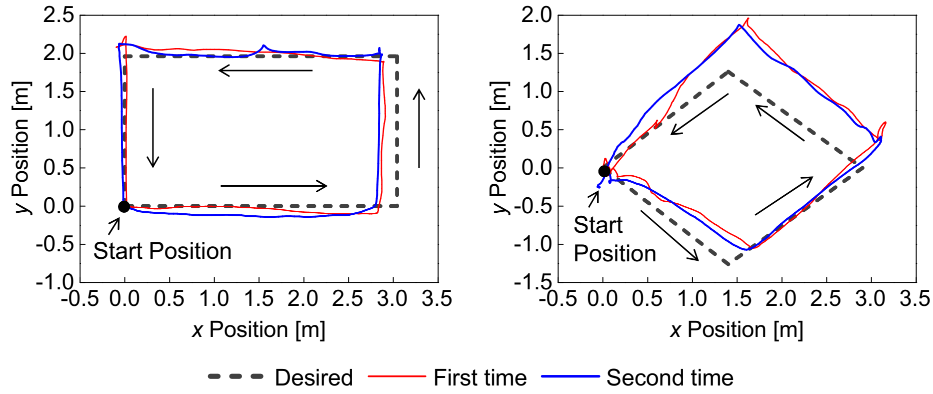

Fig. 17 Subject E's path-tracking results

obtained by several repeated experiments, although had appropriately considered the users' individual operational characteristics; some special conditions still had not be embraced. Moreover, the distance-calculation method shown in equation (2) and the reasoning method shown in equation (5) have considered all sensors in unity; in reality, each sensor has a different weight upon the effect of the reasoning results. Therefore, identification error is introduced when conducting reasoning for each direction. Furthermore, considering that backwards oblique-direction movement is uncommon for human beings, and that it is particular uncommon for them to incline their body onto the armrest, therefore, the reasoning error is larger for BL and BR direction.

In the path-tracking experiments, the identification results shown in Figs. 14 and 15 are also the same as that shown in Fig. 11. And in the path tracking results, although some tracking errors are shown in Figs. 16 and 17, the robot tracked the predesigned path with acceptable accuracy. The directional intentions of the subjects were correctly identified and properly followed by the WTR, demonstrating significant improvement over previous results [29, 32]. The intentional paths of the subject not involved in generating the fuzzy knowledge base were the same as

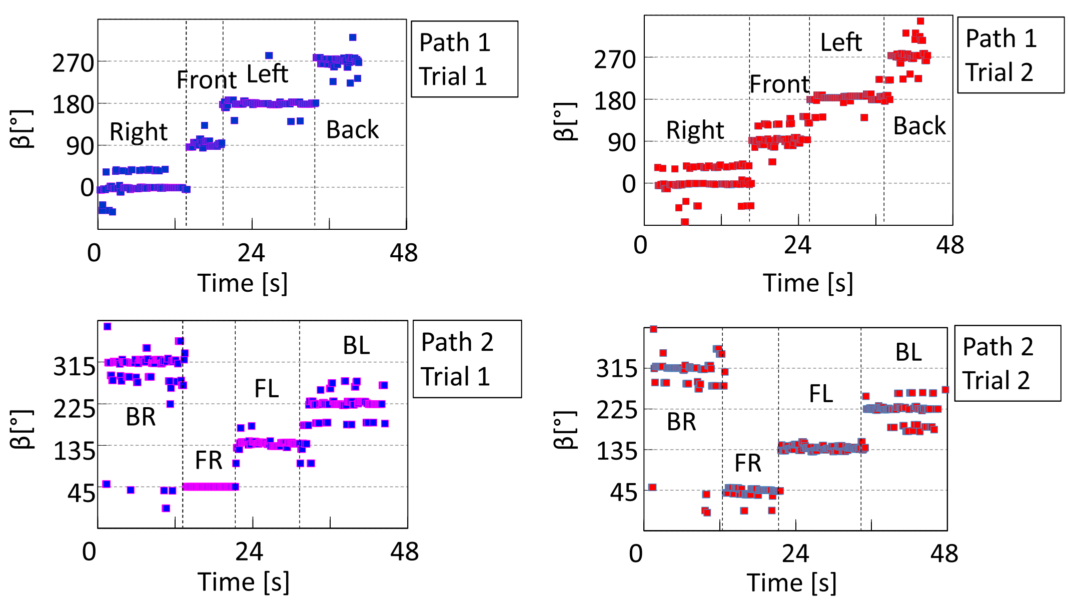

Fig. 18 Identification angles for a subject not known to the fuzzy knowledge base

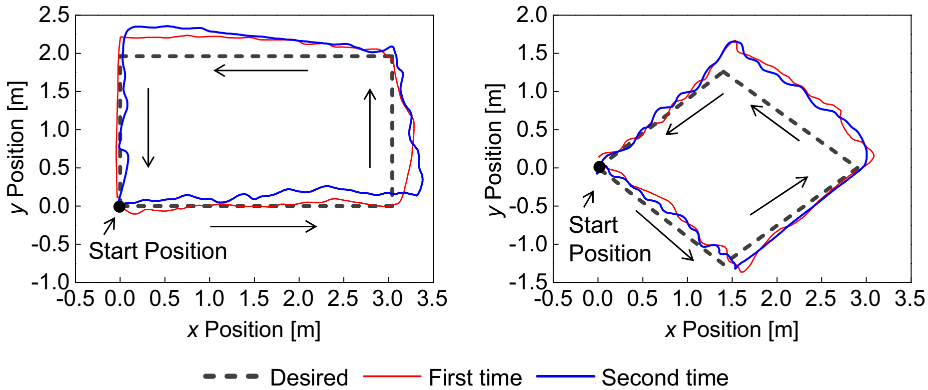

Fig. 19 Path-tracking results of a subject not involved in generating the fuzzy knowledge base

those of the other subjects shown in Figs. 18 and 19. This demonstrated that the fuzzy knowledge base was capable of guiding the WTR along the intended path of an unknown user with health conditions and walking habits similar to those of the subjects involved in generating the fuzzy knowledge base.

Overall, our experiments demonstrated that the proposed method for identifying directional intent is able to approximate the user's directional intent, that the reasoning accuracy may be optimized by adjusting the knowledge radius, and that the proposed method is able to adapt to different classes of subjects as new fuzzy knowledge sets are generated.

5 Conclusion

The novel WTR introduced in this paper will help physiotherapists administer walking training to people suffering from walking disabilities. The main contribution of this study is the proposed method for identifying a user's directional intent using a distance-type reasoning algorithm. This method can significantly increase the convenience of users and has been validated via an experiment. However, there are identification errors due to the exact of knowledge base, the reasonableness of distance calculation method, and reasoning methods. Therefore, the practicality of the proposed method is limited by the resulting low precision. Future work will attempt to improve identification accuracy by including all of the individual characteristics and special situations into the knowledge base and proposing more reasonable distance-calculation and reasoning methods. In addition, to the identification error of the BL and BR directions, other sensors, such as initial sensors and myogenic potential sensors, will be considered to increase the identification accuracy.

Although the method was validated using healthy subjects whose walking characteristics differ from those of people with walking disabilities, the method can be applied to this group by generating new fuzzy knowledge sets. In future work, experiments will be conducted with subjects who have one specific kind of walking disability by creating a new knowledge base with this kind of walking characteristic. This may confirm that the proposed method can be applied to groups of people with different walking styles.

Acknowledgment The authors would like to thank the reviewers for their constructive comments to improve the quality of the article. This work was supported by The Japan Society for the Promotion of Science KAKENHI Grant Number 21300212, 15K16401 and the Canon Foundation.

References

1. United Nations: Home-assistant robot for an aging society. Department of Economic and Social Affairs, Population Division, World Population Prospects. Revision (2015)
2. Chen, B.: Trends in disability in a super-aging society: Adapting the future elderly model to japan. In: 143rd APHA Annual Meeting and Exposition (October 31-November 4, 2015). APHA, 2015

3. Guralnik, J.M., Fried, L.P., Salive, M.E.: Disability as a public health outcome in the aging population. Annu. Rev. Public Health **17**(1), 25–46 (1996)
4. Lee, I.-M., Buchner, D.M.: The importance of walking to public health. Med. Sci. Sports Exerc. **40**(7 Suppl), S512—8 (2008)
5. Bernhardt, J., Churilov, L., Dewey, H., Lindley, R.I., Moodie, M., Collier, J., Langhorne, P., Thrift, A.G., Donnan, G.: Statistical analysis plan (sap) for a very early rehabilitation trial (avert): an international trial to determine the efficacy and safety of commencing out of bed standing and walking training (very early mobilization) within 24 h of stroke onset vs. usual stroke unit care. Int. J. Stroke **10**(1), 23–24 (2015)
6. Karttunen, A.H., Kallinen, M., Peurala, S.H., Häkkinen, A.: Walking training and functioning among elderly persons with stroke: Results of a prospective cohort study. PM&R **7**(12), 1205–1214 (2015)
7. Pyo, S.-H., Min-Gyun, O., Yoon, J.-W.: Development of an active haptic cane for gait rehabilitation. In: 2015 IEEE International Conference on Robotics and Automation (ICRA), pages 4464–4469. IEEE, p. 2015
8. Maguire, C., Sieben, J.M., Scheidhauer, H., Romkes, J., Suica, Z., de Bie, R.A.: The effect of crutches, an orthosis theratogs, and no walking aids on the recovery of gait in a patient with delayed healing post hip fracture: A case report. Physiotherapy theory and practice, p. 1–13 (2016)
9. Mun, K.-R., Guo, Z., Yu, H.: Development and evaluation of a novel overground robotic walker for pelvic motion support. In: 2015 IEEE International Conference on Rehabilitation Robotics (ICORR), p. 95–100. IEEE, p. 2015
10. Walsh, C.J., Endo, K., Herr, H.: A quasi-passive leg exoskeleton for load-carrying augmentation. Int. J. Humanoid Rob. **4**(03), 487–506 (2007)
11. Kyousuke, G., Kotani, N., Hiroyuki, F., Kazuya, S., Reiko, T., Arisa, K., Satoshi, K., Kazuhiko, S., Etuji, S., Masatoshi, N., et al.: Effectiveness of the single-joint hal®robot suit for rehabilitation after orthopedic surgery. Physiotherapy **101**, e806—e807 (2015)
12. Gupta, A., O'Malley, M.K., Patoglu, V., Burgar, C.: Design, control and performance of ricewrist: A force feedback wrist exoskeleton for rehabilitation and training. Int. J. Robot. Res. **27**(2), 233–251 (2008)
13. Meuleman, J., van Asseldonk, E., van Oort, G., Rietman, J., van der Kooij, H.: Lopes ii—design and evaluation of an admittance controlled gait training robot with shadow-leg approach (2015)
14. Jin, X., Cui, X., Agrawal, S.K.: Design of a cable-driven active leg exoskeleton (c-alex) and gait training experiments with human subjects. In: 2015 IEEE International Conference on Robotics and Automation (ICRA), p. 5578–5583. IEEE (2015)
15. Alamdari, A., Krovi, V.: Design and analysis of a cable-driven articulated rehabilitation system for gait training. Journal of Mechanisms and Robotics (2016)
16. Wang, Y., Wang, S., Tan, R., Jiang, Y., Ishida, K., Fujie, MG.: Motion control for an intelligent walking support machine. ICIC Express Lett. **6**(1), 145–149 (2012)
17. Wang, S.Y., Inoue, H., Kawata, K., Inoue, Y., Nagano, M., Ino, S., Ishida, K., Kimura, T.: Developing the omni-directional mobile walker and verifying its effect of increase in the muscle power. In: Proceedings of the JSME Symposium on Walfare Engineering, p. 176–177 (2007)
18. Mavroidis, C., Nikitczuk, J., Weinberg, B., Danaher, G., Jensen, K., Pelletier, P., Prugnarola, J., Stuart, R., Arango, R., Leahey, M., et al.: Smart portable rehabilitation devices. J. Neuroeng. Rehabil. **2**(1), 1 (2005)
19. Ishida, K., Wang, S.Y., Nagano, T., Kishi, T.: Development of an all-way mobile walker. J. Phys. Med. **19**(4), 246–250 (2008)
20. Riman, C.F., Peralta, H., Monacelli, E., Alayli, Y., Hajj, A.E., Mougharbel, I.: A multi-interface platform system for assistance and evaluation of disabled people, applied bionics and biomechanics. Appl. Bionics Biomech. **8**(1), 55–66 (2011)
21. Niazi, I.K., Mrachacz-Kersting, N., Jiang, N., Dremstrup, K., Farina, D.: Peripheral electrical stimulation triggered by self-paced detection of motor intention enhances motor evoked potentials. IEEE Trans. Neural Syst. Rehabil. Eng. **20**(4), 595–604 (2012)
22. Mellinger, J., Schalk, G., Braun, C., Preissl, H., Rosenstiel, W., Birbaumer, N., Kübler, A.: An meg-based brain–computer interface (bci). Neuroimage **36**(3), 581–593 (2007)
23. Sorger, B., Reithler, J., Dahmen, B., Goebel, R.: A real-time fmri-based spelling device immediately enabling robust motor-independent communication. Curr. Biol. **22**(14), 1333–1338 (2012)
24. Lee, J.-H., Ryu, J., Jolesz, F.A., Cho, Z.-H., Yoo, S.-S.: Brain–machine interface via real-time fmri: preliminary study on thought-controlled robotic arm. Neurosci. Lett. **450**(1), 1–6 (2009)
25. Naseer N, Hong, K.-S.: fnirs-based brain-computer interfaces: a review. Frontiers in human neuroscience, 9, 2015
26. Walter, M.R., Antone, M., Chuangsuwanich, E., Correa, A., Davis, R., Fletcher, L., Frazzoli, E., Friedman, Y., Glass, J., How, J.P., et al.: A situationally aware voice-commandable robotic forklift working alongside people in unstructured outdoor environments. J. Field Rob. **32**(4), 590–628 (2015)
27. Kofman, J., Xianghai, W., Luu, T.J., Verma, S.: Teleoperation of a robot manipulator using a vision-based human-robot interface. IEEE Trans. Ind. Electron. **52**(5), 1206–1219 (2005)
28. Bascetta, L., Ferretti, G., Rocco, P., Ardö, H., Bruyninckx, H., Demeester, E., Di Lello, E.: Towards safe human-robot interaction in robotic cells: an approach based on visual tracking and intention estimation. In: 2011 IEEE/RSJ International Conference on Intelligent Robots and Systems (IROS), p. 2971–2978. IEEE (2011)
29. Taghvaei, S., Hirata, Y., Kosuge, K.: Control of a passive walker using a depth sensor for user state estimation. In: 2011 IEEE International Conference on Robotics and Biomimetics (ROBIO), p. 1639–1645. IEEE (2011)
30. Brescianini, D., Jung, J.-Y., Jang, I.-H., Park, H.S., Robert, R.: Ins/ekf-based stride length, height and direction intent detection for walking assistance robots. In: 2011 IEEE International Conference on Rehabilitation Robotics (ICORR), pages 1–5. IEEE (2011)
31. Chan, F.H.Y., Yang, Y.-S., Lam, F.K., Zhang, Y.-T., Parker, P.A.: Fuzzy emg classification for prosthesis control. IEEE Trans. Rehabil. Eng. **8**(3), 305–311 (2000)

32. Hussein, S.E., Granat, M.H.: Intention detection using a neuro-fuzzy emg classifier. IEEE Eng. Med. Biol. Mag. **21**(6), 123–129 (2002)
33. Yokono, J., Hashimoto, S.: Center of gravity sensing for motion interface. In: 1998 IEEE International Conference on Systems, Man, and Cybernetics, 1998, vol. 2, p. 1113–1118. IEEE (1998)
34. Wasson, G., Sheth, P., Huang, C., Ledoux, A., Alwan, M.: A physics-based model for predicting user intent in shared-control pedestrian mobility aids. In: 2004 IEEE/RSJ International Conference on Intelligent Robots and Systems, 2004.(IROS 2004). Proceedings, vol. 2, p. 1914–1919. IEEE (2004)
35. Wakita, K., Huang, J., Di, P., Sekiyama, K., Fukuda, T.: Human-walking-intention-based motion control of an omnidirectional-type cane robot. IEEE/ASME Trans. Mechatron. **18**(1), 285–296 (2013)
36. Bello, O., Holzmann, J., Yaqoob, T., Teodoriu, C.: Application of artificial intelligence methods in drilling system design and operations: a review of the state of the art. Journal of Artificial Intelligence and Soft Computing Research **5**(2), 121–139 (2015)
37. Raza, M.Q., Khosravi, A.: A review on artificial intelligence based load demand forecasting techniques for smart grid and buildings. Renew. Sust. Energ. Rev. **50**, 1352–1372 (2015)
38. Valipour, M., Banihabib, M.E., Behbahani, S.M.R.: Comparison of the arma, arima, and the autoregressive artificial neural network models in forecasting the monthly inflow of dez dam reservoir. J. Hydrol. **476**, 433–441 (2013)
39. Valipour, M.: Optimization of neural networks for precipitation analysis in a humid region to detect drought and wet year alarms. Meteorol. Appl. **23**(1), 91–100 (2016)
40. Valipour, M.: Sprinkle and trickle irrigation system design using tapered pipes for pressure loss adjusting. J. Agric. Sci. **4**(12), 125 (2012)
41. Khasraghi, M.M., Sefidkouhi, M.A.G., Valipour, M.: Simulation of open-and closed-end border irrigation systems using sirmod. Arch. Agron. Soil Sci. **61**(7), 929–941 (2015)
42. Valipour, M., Sefidkouhi, M.A.G., Eslamian, S.: Surface irrigation simulation models: a review. International Journal of Hydrology Science and Technology **5**(1), 51–70 (2015)
43. Adăscăliţei, F., Doroftei, I.: Practical applications for mobile robots based on mecanum wheels-a systematic survey. Gh. Asachi Technical University of Iasi, Mechanical Engineering Faculty, Theory of Mechanisms and Robotics Department, B-dul D, Mangeron, p. 61–63 (2011)
44. Wang, Y., Wang, S., Tan, R., Jiang, Y., Ishida, K., Fujie, M.G.: Improving the motion performance for an intelligent walking support machine by rls algorithm. ICIC Express Lett. **7**(4), 176–177 (2013)
45. Mamdani, E.H.: Application of fuzzy algorithms for control of simple dynamic plant. In: Proceedings of the Institution of Electrical Engineers, volume 121, pages 1585–1588. IET (1974)
46. Takagi, T., Sugeno, M.: Fuzzy identification of systems and its applications to modeling and control. IEEE Trans. Syst. Man Cybern. **1**, 116–132 (1985)
47. Maeda, M., Murakami, S.: A self-tuning fuzzy controller. Fuzzy Sets Syst. **51**(1), 29–40 (1992)
48. Mizumoto, M., Zimmermann, H.-J.: Comparison of fuzzy reasoning methods. Fuzzy Sets Syst. **8**(3), 253–283 (1982)
49. Mizumoto, M.: Fuzzy controls under various fuzzy reasoning methods. Inf. Sci. **45**(2), 129–151 (1988)
50. Wang, S., Tsuchiya, T., Mizumoto, M.: Distance-type fuzzy reasoning method. Journal of Biomedical Fuzzy Systems Association **1**(1), 61–78 (1999)
51. Chaudhur, B.B., Rosenfeld, A.: On a metric distance between fuzzy sets. Pattern Recogn. Lett. **17**(11), 1157–1160 (1996)
52. Lindblad, J., Sladoje, N.: Linear time distances between fuzzy sets with applications to pattern matching and classification. IEEE Trans. Image Process. **23**(1), 126–136 (2014)

Yina Wang received the PhD in engineering from Kochi University of Technology, Japan, in 2014. She is currently a research associate at the Kochi University of Technology. Her current research interests include control engineering, robotics, and computational intelligence. She is a member of the IEEE, the Japan Society of Mechanical Engineering (JSME), the Robotics Society of Japan, and the Japanese Society for Medical and Biological Engineering.

Shuoyu Wang received the Ph.D. degree in Electrical Engineering from Hokkaido University, Sapporo, Japan, in 1993. He is Professor in the School of Systems Engineering, Kochi University of Technology. His current research interests are walking rehabilitation robots, control, and fuzzy reasoning. Dr Wang is a fellow of the Japan Society of Mechanical Engineering (JSME), and a member of the IEEE, the Society of Instrument and Control Engineers, the Robotics Society of Japan, the Japanese Society for Medical and Biological Engineering, and the Japan Society for Fuzzy Theory and Intelligent Informatics.